JJEE
Volume 9 | Number 4 | December 2023 | Pages 566-590

Jordan Journal of Electrical Engineering

ISSN (print): 2409-9600, ISSN (online): 2409-9619

Homepage: jjee.ttu.edu.jo

An Integrated Approach for Yaw Stability of Linear Time Varying Bicycle Model Utilizing Adaptive Model Predictive Control

Rahul Prakash[1], Dharmendra Kumar Dheer[2*]

[1, 2] Department of Electrical Engineering, National Institute of Technology Patna, Bihar, India
E-mail: dkdheer@nitp.ac.in

Received: February 11, 2023 *Revised: May 01, 2023* *Accepted: May 08, 2023*

***Abstract*—** Accidents during critical maneuvering on roads while overtaking or changing lanes are mainly due to the insufficient generation of the stability matrices of vehicles, including yaw rate. The parameters responsible for stable operation of the vehicle during these driving scenarios may vary, causing improper steering angle input actuation to the vehicle, due to which the desired yaw rate is not generated. To overcome this problem, corrective yaw moments are applied to the yaw dynamics to generate the desired yaw rate and operate the vehicle within the defined stability limit. Therefore - in this paper - to improve the yaw stability of the vehicle, a novel yaw rate gradient-based control approach is proposed for a linear time-varying (LTV) bicycle model. A 2 degrees of freedom bicycle model with the linear approximation for low slip angles in the magic formula tire model is utilized to develop the LTV model. The longitudinal velocity and friction coefficient are chosen as the parameters of interest to be varied during model simulation. Two different critical driving scenarios, including a sine maneuver and a double lane change, are chosen as input actuation with and without corrective yaw moments. The obtained simulation results unveil that, by the application of steering angle with a corrective yaw moment, the yaw stability has effectively been improved by obtaining a feasible adaptive model predictive control solution. Additionally, the root mean square error (RMSE) is calculated to evaluate the performance of the proposed methodology. A RMSE of 0.0768 and 0.0395 for steering without corrective yaw moment (CYM) is decreased to 0.0234 and 0.0214 for sine and double lane change steering input with CYM, respectively. Moreover, the proposed methodology is compared with previous methods and found to have better yaw stability.

***Keywords*—** Front steering; Corrective yaw moment; Bicycle model; Adaptive model predictive control; Yaw stability; Linear time varying model.

1. INTRODUCTION

Vehicle lateral control systems are implemented in the automotive industry to address the lane keeping system and avoid accidents during lane departures. The yaw stability control system is one of the lateral control systems and is a major challenge in commercial vehicles. In the recent years, yaw control systems or electronic stability control systems have been developed and recently commercialized by several automotive manufacturers to prevent vehicles from spinning and drifting out. Due to high vehicle velocity or a low friction coefficient, it is difficult for the vehicle to respond to the driver's steering input, as described in [1]. In [2], authors proposed a prioritization-based control structure for improving the vehicle's yaw stability for different slippery conditions. An electronic limited slip differential (ELSD) clutch pressure on the rear axle and differential braking control actuations are designed and are activated if the yaw rate consFtraints are violated.

* Corresponding author
Article's DOI: 10.5455/jjee.204-1676111104

For lateral stability of the nonlinear vehicle, active front steering (AFS) and differential braking (DB)-based nonlinear model predictive control (NMPC) control strategies are designed for various parameters and states with constant steering angle and double lane change manoeuvre with different road friction [3]. In [4], an integrated control of AFS and direct yaw control (DYC) strategy is proposed for energy efficiency and lateral stability for various steering inputs, including sine, single lane change, and slalom manoeuvres. A terminal sliding mode control and a LTV-MPC controller are designed to reduce additional yaw moment during cornering. Authors in [5] proposed an approach to stabilize the vehicle yaw and lateral motion by designing a new LTV-MPC for a 2 degrees of freedom (DOF) model utilizing the sine and double lane change manoeuvre. The nonlinear behaviour of the tire is simplified by two straight lines to implement the linear characteristics and ease the calculation complexity. In [6], a MPC based integrated control of AFS and DYC for lateral stability of vehicle considering stability margin is implemented. A combination of AFS and DYC is applied to improve the handling stability of a 2 DOF nonlinear vehicle model by incorporating the change in cornering stiffness of tires by the authors in [7].

Authors in [8] have proposed a coordinated control by designing a hybrid MPC based on the 2 DOF model in terms of slip angles to achieve better yaw stability and faster convergence. An adaptive MPC is designed for an 8 DOF nonlinear vehicle model, utilizing an integrated control of steering and yaw control methods for J-turn and double lane change manoeuvre [9]. In emergency situations, the steering angles are not enough to generate the required lateral tire forces to track the curvature. Thus, to avoid sudden obstacles, in [10], authors proposed integrated steering and differential braking based on MPC to encounter such situations. Authors in [11] have proposed a novel 2 stage process of an emergency steering assist system that provides steering input and differential braking for stability of rear end collision avoidance in highway driving. To enhance the lateral stability while maximizing the velocity in cornering, an integrated chasis control of differential braking, traction torque, and roll moment has been designed by the authors in [12]. A coordinated chasis control is designed by utilizing a differential braking, traction distribution, and steering system for 4 wheel drive vehicle to improve the handling stability during cornering [13].

Authors in [14] have proposed a manoeuvre stability controller based on MPC to enhance the performance of steering control actuation with lateral stability based on a 2 DOF vehicle model. In [15], an evasive steering based control is designed by considering the motor voltage, actuator bandwidth, and disturbances using MPC. A dual sliding mode controller is designed to enhance the stability and handling of 4 WID-EVs, the integrated control of steering and direct yaw control is employed by the authors in [16]. A lateral tire force and sideslip angle observer based direct yaw control is proposed in [17], to improve stability at high speed cornering. In [18], to enhance the lateral stability, a sliding mode variable structure control is designed for the additional yaw moment on icy asphalt road conditions. For improving the lateral stability during cornering, the problems of adhesion constraint, model uncertainty, and external disturbance in the active steering system are addressed by the authors in [19] by minimizing the cost function of MPC with respect to the steering input. In [20], authors have proposed dual LMPC and LTV-MPC to handle the nonlinear characteristics of the tire forces. The control strategy enhances the capability of active front steering input and maintains yaw stability within the handling limits. In [21], a slide mode and back

stepping control strategy are proposed for the improvement of handling stability by utilizing active suspension system with steering and differential braking. For fault detection in the steering system, the authors in [22] proposed an adaptive MPC to avoid roll over and improve the lateral stability. In [23], a segmented coordinated control based on steering and differential braking is proposed based on the fuzzy controller to improve the lane departure system. Authors in [24] have proposed an adaptive neuro fuzzy inference systems 2 based back-stepping sliding model control for the improvement in stability due to the presence of uncertainty in nonlinear systems. In [25], a method is developed for analyzing the stability of adaptive fuzzy logic controllers (AFLC) systems using robust stability and robust performance criteria. The results show that developed method can be applied for the design of a robust FLC systems that compete with adaptive counterparts.

Based on the rigorous literature survey, authors have identified the research gaps that are yet uncovered and are described here. In most of the research works, the mathematical models proposed for yaw stability are more than a 2 DOF nonlinear model [26]. Also, the noises are explicitly added in the state space model to observe the effect of external disturbance (the sudden appearance of obstacles and the dryness of the surfaces changing). These proposed methods for the modelling, results in more mathematical complexity, constraints that conflict while designing the controller, and a high computational load for a model predictive controller. The conflicts of the constraints give rise to infeasible solution. Secondly, in the literature it is found that, the control steering input is activated to achieve yaw stability, if the measured yaw rate is at the extreme values of the defined stable boundary limits. Due to this, if a small input disturbance, such as a sudden obstacle appearance or change in parameter occurs. It can lead the measured yaw rate to fall into the region of instability, which may cause a collision with an obstacle or improper yaw motion, and the vehicle goes off the defined reference trajectory.

The problems identified in the literature are related to the stable operation of the vehicle during its running on the road to avoid collision with other vehicles and follow the defined trajectory for different input steering [27]. The yaw rate of the vehicle is a stability matrix that provides information on the spinning of the vehicle during cornering maneuvers. A yaw rate value higher than the defined boundary limits leads to spinning of the vehicle with respect to the vertical axis, resulting in instability. In trajectory tracking, the steering angle is responsible for providing the required lateral tire force for lateral agility. This lateral tire force generates the required yaw moment ($l_f F_{yf} - l_r F_{yr}$). Due to the continuously changing parameters, it may be possible that the yaw moment is insufficient for lateral agility. In this case, a corrective yaw moment is generated by differential braking to improve lateral stability and avoid sudden obstacles.

Therefore, this study proposes a novel methodology to solve the problems identified. The contributions made by the authors to fill the research gap in the literature so far are mentioned here. Firstly, to solve the problems identified, a 2 DOF LTV model is developed with lesser number of constraints. The noises in the system are modelled as the effect of external disturbances resulting in parameter variations, thus developing a simplified linear dynamic model. Secondly, the yaw stability limit of a vehicle is described by the bounding of the yaw rate, which depends on longitudinal velocity and friction coefficient. The variations implemented in these parameters led to the development of a linear time varying (LTV)

model. Lastly, a novel yaw rate gradient-based input weight prioritization of AMPC is proposed to activate the corrective yaw moments. This enforces the yaw rate to stay within the limits and the vehicle to show oversteer behaviour, thus improving the yaw stability.

Further, the paper is organised as: In section 2, the mathematical model of the vehicle is presented. The control strategy for the yaw stability of model is described in section 3. Simulation results and discussion are presented in the section 4. Finally, the conclusions are presented in section 5.

2. MATHEMATICAL MODEL

The desired yaw rate and the sideslip angle are calculated with respect to the provided input steering angle in the simulation. A linear 2 DOF bicycle model is adopted to develop the mathematical model of the vehicle as shown in Fig. 1.

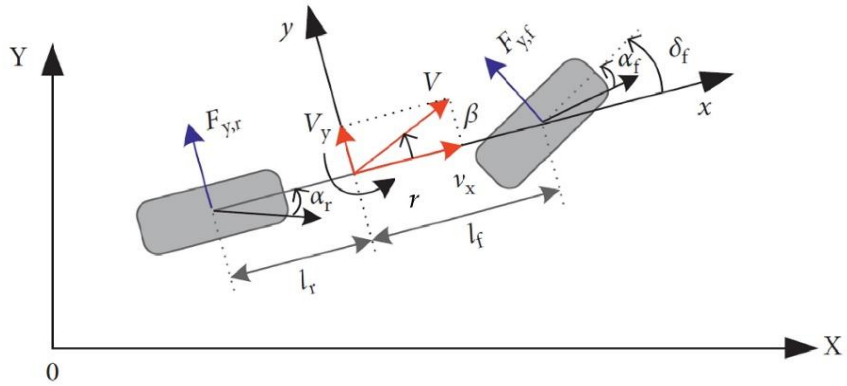

Fig. 1. The bicycle model.

This is a front wheel drive model in which steering angle is provided only to the front wheel. This is a steady state vehicle model obtained by linearizing the lateral force and neglecting the lateral weight transfers and roll dynamics. The longitudinal velocity and friction coefficient are the parameters of interest to analyze the proposed controller performance for the model. The model is created by utilizing sideslip angle (β) and yaw rate (r) as state variables. To improve the yaw stability, a corrective yaw moment (M_z) is added to the yaw dynamics. The dynamical equations for the model adopted [10, 28] are described as:

$$\dot{\beta} = \frac{1}{mV_x}(F_{yf} + F_{yr}) - r, \tag{1}$$

$$\dot{r} = \frac{1}{I_z}\left(l_f F_{yf} - l_r F_{yr} + M_z\right) \tag{2}$$

where $\beta = tan^{-1}(v_y/v_x)$ is the sideslip angle of the vehicle at the center of gravity (CG), r is the yaw rate, m is the mass of the vehicle, V_x is the longitudinal velocity, l_f is the distance of the front axle from CG, l_r is the distance of the rear axle from CG, M_z is the corrective yaw moment, I_Z is the moment of inertia, F_{yf} and F_{yr} are the front and rear lateral tire forces. This study utilizes the magic formula tire model for determining the tire lateral forces [28].

$$F_y = \mu D sin\{Carctan[B\alpha - E(B\alpha - arctan(B\alpha))]\} \tag{3}$$

$$C = a_0, \quad D = (a_1 F_z^2 + a_2 F_z)$$
$$B = \frac{a_3 sin[arctan(F_z/a_4)]}{CD} \tag{4}$$

where μ is the friction coefficient, Tire force F_y is approximated as $BCD\alpha$ as mentioned in [29] for a linear range with respect to small slip angles. The product BCD is a constant and is assumed as C_α. Different road conditions are represented by involving different values of μ.

$$F_{yf} = \mu BCD\alpha_f, \quad F_{yr} = \mu BCD\alpha_r \tag{5}$$

$$\alpha_f = \left(-\delta + \beta + \frac{\boldsymbol{l_f r}}{V_x}\right), \quad \alpha_r = \left(\beta - \frac{l_r r}{V_x}\right) \tag{6}$$

F_z is the total vertical static load of the vehicle. The load is taken to be distributed between the front and rear wheels based on the geometry of the vehicle model [5]:

$$F_{zf} = \frac{mgl_r}{l_f + l_r}, \quad F_{zr} = \frac{mgl_f}{\boldsymbol{l_f + l_r}} \tag{7}$$

Front and rear tire lateral forces are defined as:

$$F_{yf} = \mu C_{\alpha_f}\alpha_f, \quad F_{yr} = \mu C_{\alpha_r}\alpha_r \tag{8}$$

where,

$$C_{\alpha_f} = B_f CD_f, \tag{9}$$

$$C_{\alpha_r} = B_r CD_r \tag{10}$$

The lateral acceleration of the vehicle is bounded by the equation defined as:

$$a_y \leq \mu g \tag{11}$$

Fig. 2 shows the linear region of the lateral force (F_y) for the small slip angle. The variation in the lateral forces with respect to the different μ and V_x are also shown. The front lateral force experienced by the tires increases as the friction coefficient increases. Further, Eq. (8) is placed in the model defined by the Eqs. (1) and (2), to be represented in state space form. The state space form is given by the Eq. (12):

$$\dot{x}(t) = A_c x(t) + B_c u(t), \quad y(t) = C_c x(t) \tag{12}$$

where A_c, B_c, and C_c are the system matrices developed for LTI and LTV model defined in later sections.

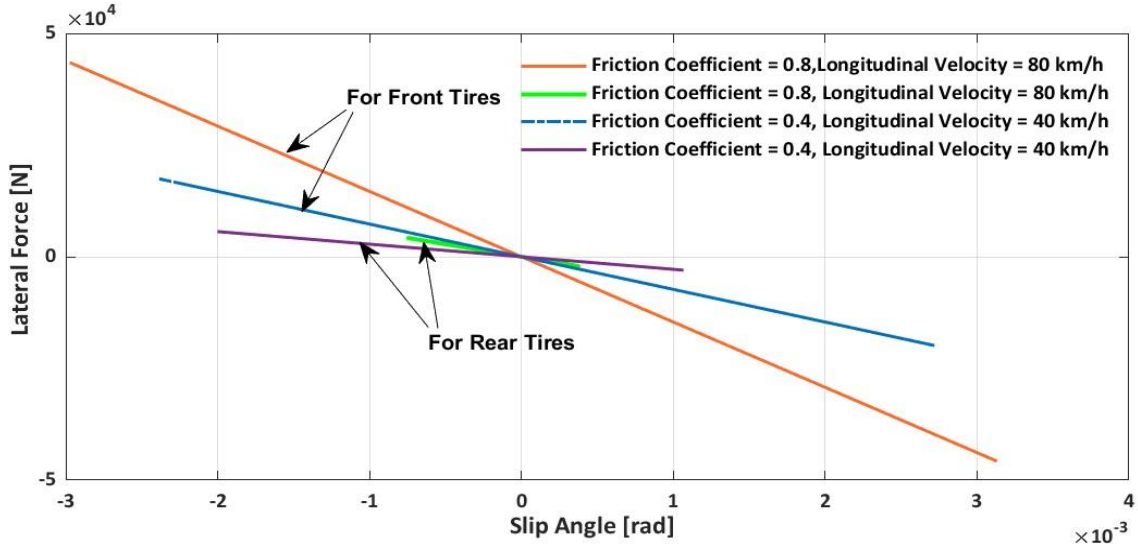

Fig. 2. Lateral tire forces.

2.1. LTI Model

In this section, the LTI model of the vehicle is developed using Eq. (12) [5]. The corrective yaw moment M_z in Eq. (2) is ignored for this LTI model. Therefore, in the state space dynamics of the vehicle represented by Eq. (12), the matrices defined are invariant over

time as parameters are chosen to be constant. The states and input for the model are defined as $x = [\beta\ r]', u = [\delta]$. The LTI model is obtained by placing the lateral forces mentioned in Eq. (8) into Eqs. (1) and (2). The model obtained is described in Eqs. (13) to (15):

$$A_c = \begin{bmatrix} \frac{\mu(C_{\alpha_f}+C_{\alpha_r})}{mV_x} & \frac{\mu(l_rC_{\alpha_r}-l_faC_{\alpha_f})}{mV_x^2} - 1 \\ \frac{\mu(l_rC_{\alpha_r}l_fC_{\alpha_f})}{I_z} & -\frac{\mu(l_f^2C_{\alpha_f}+l_r^2C_{\alpha_r})}{V_xI_z} \end{bmatrix} \quad (13)$$

$$B_c = \begin{bmatrix} -\frac{C_{\alpha_f}}{mVx} \\ -\frac{l_fC_{\alpha_f}}{I_z} \end{bmatrix} \quad (14)$$

$$C_c = \begin{bmatrix} 1 & 0 \\ 0 & 1 \end{bmatrix} \quad (15)$$

where A_c is the state matrix representing the dynamics of the vehicle, B_c is the input matrix, and C_c is the output matrix. In this model, the longitudinal velocity and friction coefficient are assumed to be constant over time thus, representing that there is no obstacles in the track of vehicle or no acceleration and brakes are applied. The road surface is also assumed not to vary from dry to wet or vice versa, representing a constant friction coefficient.

2.2. LTV Model

In the LTI model, the system dynamics do not change with time, which is not practical, and tracking of the reference variables is due to steering angle only. To develop the LTV model, the authors in this study considered the uncertainty in the parameters as variations due to the presence of external disturbance, including the sudden appearance of an obstacle on the path or variations in the road surface. An LTV model is developed by varying the parameters V_x and μ in LTI model such that disturbances are experienced without explicitly adding additional noise signal making the model complex.

The model in Eqs. (16) to (18) represent the linear time varying characteristics due to the inclusion of variations in the domain of the parameters. In this model, a condition based input is given to the system to analyze the combined effect of steering input and corrective yaw moments. The selection of the input matrix $B_c(k)$ is based on the weight matrix in the MPC controller.

$$A_c(k) = \begin{bmatrix} \frac{\mu(k)(C_{\alpha_f}+C_{\alpha_r})}{mV_x(k)} & \frac{\mu(k)(l_rC_{\alpha_r}-l_fC_{\alpha_f})}{mV_x^2(k)} - 1 \\ \frac{\mu(k)(l_rC_{\alpha_r}l_fC_{\alpha_f})}{I_z} & -\frac{\mu(k)(l_f^2C_{\alpha_f}+l_r^2C_{\alpha_r})}{V_xI_z} \end{bmatrix} \quad (16)$$

$$B_c(k) = \begin{cases} \begin{bmatrix} -\frac{C_{\alpha_f}}{mVx(k)} & 0 & 0 \\ -\frac{l_fC_{\alpha_f}}{I_z} & \frac{1}{I_z} & \frac{1}{I_z} \end{bmatrix}, & \text{if} -\Delta r_{max} \geq \Delta r \geq \Delta r_{max} \quad (17.a) \\ \begin{bmatrix} -\frac{C_{\alpha_f}}{mVx(k)} & 0 & 0 \\ -\frac{l_fC_{\alpha_f}}{I_z} & 0 & 0 \end{bmatrix}, & \text{otherwise} \quad (17.b) \end{cases}$$

$$C_c = \begin{bmatrix} 1 & 0 \\ 0 & 1 \end{bmatrix} \quad (18)$$

where m and I_z are the vehicle mass and the yaw inertia, l_f and l_r denotes the distances from the front and the rear axles to CG, δ is the steering angle, M_z is the corrective yaw moment, $M_z = M_{zf} + M_{zr}$ with M_{zf} and M_{zf} are the front and the rear differential braking, $C_{\alpha f}$ and $C_{\alpha f}$ are the front and the rear cornering coefficient.

A novel gradient-based input weight matrices method for AMPC is proposed to achieve yaw stability. In this method, the rate of change (gradient) of actual states is monitored and if required, a corrective yaw moment is activated as an additional control actuation with steering angle. The gradient of yaw rate is calculated, then, based on the calculated gradient, the input matrix is prioritized to suppress the yaw rate before diverging into the region of instability by the activation of CYM. If the value of the gradient is above a threshold value, then from Eqs. (19) and (17.a), the steering angle is prioritized with CYM. If the value of the gradient is below the threshold value, then only the steering angle is activated to control the yaw dynamics defined by Eqs. (20) and (17.b). A brief description of the proposed methodology is given in next section. The input weight matrix of AMPC is designated as W_{3inp}, otherwise W_{1inp} defined as:

$$W_{3inp} = \begin{bmatrix} W_{\Delta u} & 0 & 0 \\ 0 & W_{M_{zf}} & 0 \\ 0 & 0 & W_{M_{zr}} \end{bmatrix} \quad (19)$$

$$W_{1inp} = \begin{bmatrix} W_{\Delta u} & 0 & 0 \\ 0 & 0 & 0 \\ 0 & 0 & 0 \end{bmatrix} \quad (20)$$

The profiles of longitudinal velocity and friction coefficient are chosen to experience practical situations. The profile of V_x and μ can be realized as the vehicle is travelling from a wet road to a dry and then back to wet surface, thus the velocity is chosen to be first increasing and then decreasing. If the longitudinal velocity is high on a wet road then the vehicle will not be able to track the nominal yaw rate. Figs. 3 and 4 depict the variation profiles of both variables. From the figure, it is evident that a sufficient variation range is opted to analyze the performance of the controller.

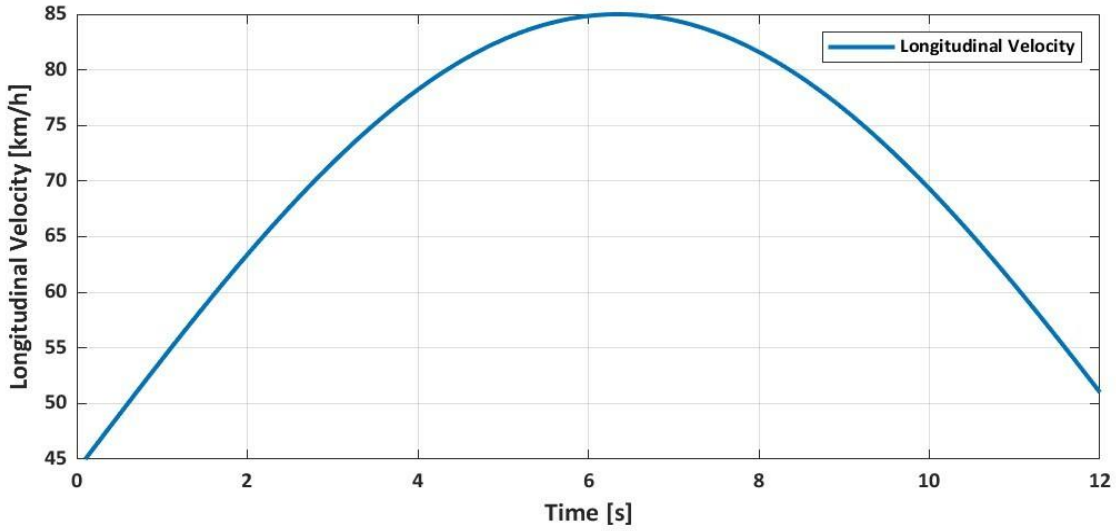

Fig. 3. Profile of the longitudinal velocity.

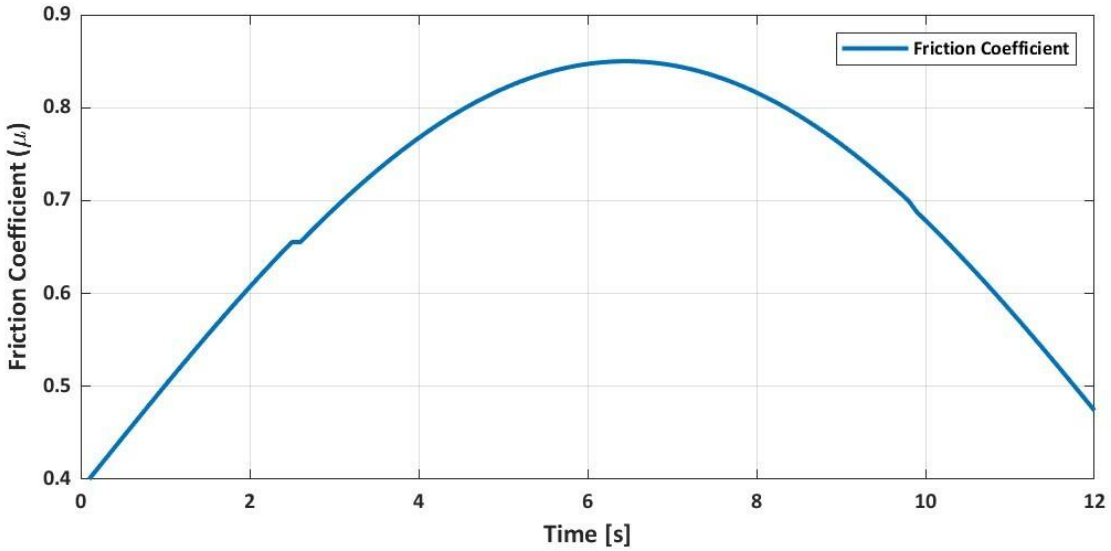

Fig. 4. Profile of the friction coefficient.

3. CONTROL STRATEGY

Firstly, a LTI MPC is developed considering the stability limits of the vehicle. For yaw stability, only the steering angle is implemented as an input in the LTI model. The controller is designed to operate at a specific value of longitudinal velocity and friction coefficient. The variations in the system parameters influence the controller's performances, leading to the shifting of the vehicle state beyond the stable boundary. Due to this, the vehicle becomes unstable and performs abruptly and the safety deteriorates. An adaptive MPC can address this degradation by adapting the prediction model for the changing operating conditions of nonlinear or time-varying plant characteristics. In the adaptive MPC, as time evolves the nominal operating point is updated to be consistent with the updated plant model. Therefore, a model update algorithm based adaptive MPC is developed to incorporate the continuously varying parameter characteristics to limit the states inside the boundary and stabilize the vehicle.

Fig. 5 shows the block diagram for the proposed methodology for integrated actuator control based on AMPC. The block of variable parameters comprises the longitudinal velocity and the friction coefficient with profile as shown in Figs. 3 and 4 respectively. A continuously changing parameters is fed to the vehicle mathematical model governed by Eqs. (1) and (2), which is shown by the plant block. At the same time, information about the parameters is also sent with the model update block. This block requires information about current states from the vehicle mathematical model and manipulated variables to generate the updated model for the AMPC which is governed by Eq. (35). The output of the updated model is the prediction model defined by Eq. (32). The reference block sends the updated reference signal by utilizing the different input steering. The reference values are defined by Eqs. (39) and (40) to the AMPC to solve the cost function. As the adaptive MPC requires an updated model at each time step, therefore, the model update block is connected to the AMPC. The outputs from the vehicle are measured and feedback to the controller to calculate the cost function of AMPC. The gradient of the yaw rate (Δr) is monitored continuously for comparison with the defined threshold value. If the gradient value is outside the defined range, then the weight matrix assigned to the cost function of AMPC is

defined by Eq. (17.b) and the input matrix is selected by Eq. (20). Therefore, the steering angle is generated without CYM. If the gradient of the yaw rate (Δr) crosses the threshold value, then weight matrix is assigned to cost function is defined by Eq. (17.a) and the input matrix is described by Eq. (19) and the manipulated variable is obtained as steering input with CYM. Thus, the AMPC solves the cost function described by Eq. (34). The threshold value of the gradient to be satisfied is obtained after many trials and error to find the better control of yaw rate.

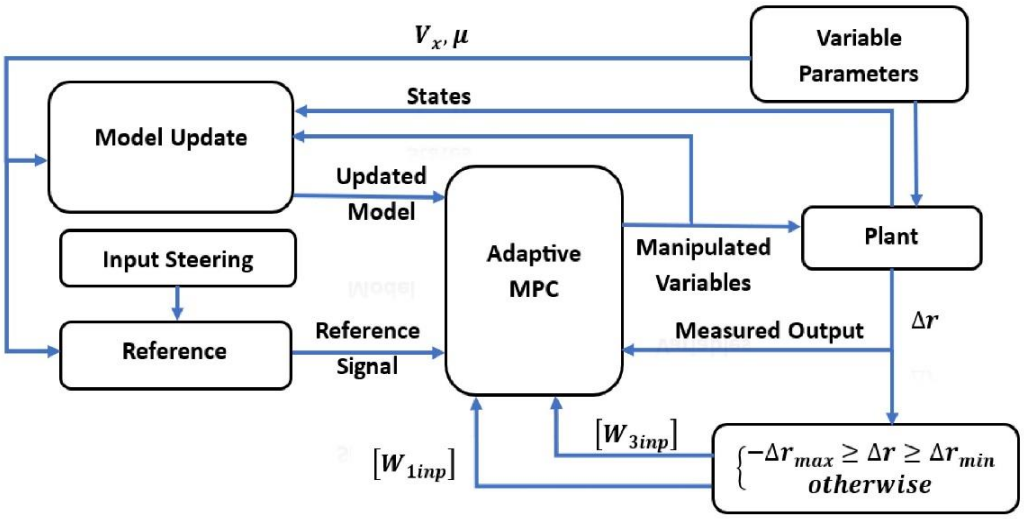

Fig. 5. Block diagram of the proposed control strategy.

If the steering angle is found to be insufficient to bound the variables inside the stable limit and the slope of the actual rate exceeds a specified value; then, the corrective yaw moments are activated to constraint the vehicle inside the stable limit for the different combination of longitudinal velocity and friction coefficient as shown in the simulation results section. The yaw rate is represented by the blue dotted line in Figs. 7 and 19 for both steering inputs without CYM, and the brown solid line represents the yaw rate for the steering input with CYM. Figs. 8(a), 8(b), 16(b) and 16(c) respectively represent the activation of CYM following the condition given by Eq. (17). For the gradient of yaw rate from Figs. 7 and 19 higher than the threshold value results in activation of CYM for both sine and double lane change steering inputs.

3.1. MPC Cost Function Formulation

Model predictive controllers are exploited for controlling the input actuations due to their explicitly constraints handling characteristics. The model described in Eq. (12) is a continuous multi-input multi-output system. The system to be controlled is usually modelled in a discrete state space model for the MPC as mentioned in the literature [28, 29]. Eq. (12) is transformed into a discrete state-space model.

$$x_d(k+1) = A_d x_d(k) + B_d u_d(k) \quad (21)$$
$$y_d(k) = C_d x_d(k)$$

The discrete model demonstrated in Eq. (21) is obtained by the Euler method for discretization. The discrete matrices are mentioned in Eqs. (22) to (24):

$$A_d = e^{A_c \Delta T}, \quad (22)$$

$$B_d = \int_0^T e^{A_c \Delta T} B_c dt \quad (23)$$

$$C_d = C_c \quad (24)$$

where A_d, B_d represents the discrete state and control matrices respectively are obtained by discretizing at the sample time of T_s = 0.1s to be utilized by the model predictive controller.

The augmented form of the model defined by Eq. (21) is obtained by considering the difference of the state variables and the control variables defined as:

$$\Delta x_d(k+1) = x_d(k+1) - x_d(k) \quad (25)$$

$$\Delta x_d(k+1) x_d(k) - x_d(k-1) \quad (26)$$

$$\Delta u(k) = u(k) - u(k-1) \quad (27)$$

The incremented state space form is represented by Eq. (28) as:

$$x_a(k+1) = A_a x_a(k) + B_a \Delta u(k) \quad (28)$$

$$y_a(k) = C_a x_a(k)$$

where the discrete augmented matrices A_a, B_a, and C_a are obtained by equations defined in [29].

The prediction model for the MPC is described as [30, 31]:

$$y(k) = Fx(k) + G\Delta u(k) \quad (29)$$

where F and G matrices are the LTI system dependent matrices. Eq. (29) is implemented to obtain the cost function satisfying the constraints of the MPC defined later.

Now, to formulate an adaptive MPC mentioned in [32, 33], the continuous time LTV model is defined by Eq. (30):

$$\dot{x}_c(t) = A_c(t)x(t) + B_c(t)u(t) \quad (30)$$

$$y_c(t) = C_c x(t)$$

Further, Eq. (30) is discretized by using Eqs. (22) to (24) and by replacing the time invariant matrix with $A_c(k)$, $B_c(k)$. Eq. (31) below represents the augmented LTV model as:

$$x_a(k+1) = A_a(k)x_a(k) + B_a(k)\Delta u(k) \quad (31)$$

$$y_a(k) = C_a x_a(k)$$

The AMPC cost function is designed while satisfying the constraints on inputs and outputs. The LTV prediction model for adaptive MPC is defined by Eq. (32):

$$y(k) = F(k)x(k) + G(k)\Delta u(k) \quad (32)$$

where $F(k)$ and $G(k)$ are the system matrices obtained from the augmented model represented by Eq. (31). Eqs. (29) and (32) are implemented to obtain the cost function for MPC and AMPC respectively defined in Eq. (33) described as:

$$J(\Delta(k), n, p) = \sum_{n=1}^{p} \left|\left|W_y\left(y(k+i|k) - r(k+i|k)\right)\right|\right|^2 + \sum_{n=1}^{n} ||W_{\Delta u}\Delta u(k+i-1)||^2 \quad (33)$$

This cost function can be further represented as:

$$J = (R-Y)^T W_y (R-Y) + \Delta U^T W_{\Delta u} \Delta U \quad (34)$$

where $W_{\Delta u}$ can be W_{3inp} *or* W_{1inp} as described in the control strategy section. An adaptive MPC is implemented to handle the linear time varying parameters of the vehicle model [32, 33]. At each control interval, the adaptive MPC controller updates the plant model and nominal operating conditions. Once updated, the model and conditions remain constant over the prediction horizon. The updated discrete plant model and nominal operating conditions required by adaptive MPC are defined by Eq. (35):

$$A_a(k+1) = A_a(k)$$
$$B_a(k+1) = B_a(k)$$
$$C_a(k+1) = C_c(k)$$
$$x_a(k+1) = x_a(k)$$
$$\Delta u(k+1) = \Delta u(k)$$
$$y_a(k+1) = y_a(k)$$
$$Dx_a(k+1) = A_a(k)x(k) + B_a(k)\Delta u(k) - x(k) \quad (35)$$

Utilizing Eq. (35), the plant model and the operating condition required by the adaptive MPC are updated at each time step. The previous time step values of the states are obtained from the plant model and the augmented discrete variable system matrices $A_a(k)$, $B_a(k)$ and $C_a(k)$ are calculated with the help of the parameters of interest fed to the model updating block. Consequently, the QP problem defined by the cost function represented by Eq. (34) of the AMPC will be adapted to updated model given by Eq. (35) at each sampling interval.

3.2. MPC Constraints Formulation

The constraints on input $u = \delta$, the increment in input $\Delta u = \Delta\delta$, and output $y = [\beta\ r]$ are defined as:

$$u_{min} \le u \le u_{max}, \quad (36)$$
$$\Delta u_{min} \le \Delta u \le \Delta u_{max} \quad (37)$$

The output constraints are described as:

$$y_{min} \le y \le y_{max} \quad (38)$$

where W_y and W_u are the positive definite weight matrices of output and input increments respectively. The model output, reference values, and inputs are designated as y, r, Δu respectively. The control horizon is n and prediction horizon is p with $n \le p$ [28]. The objective of MPC is to generate the control sequence by minimizing the cost function defined by Eq. (34) subject to input constraints Eqs. (36) and (37), output constraints Eq. (38), and vehicle dynamics Eqs. (1) and (2).

The controller's purpose is to improve the yaw stability by tracking desired values and enforcing to stay inside the stability limit. To ensure the lateral stability of the vehicle, a stability constraint on the vehicle yaw rate and sideslip angle can be defined [9]. The steady state assumption for vehicle lateral dynamics, Eqs. (1) and (2), is exploited to define the stable bound of yaw rate and sideslip angle. The reference values of angle yaw rate and sideslip angle are described as follows:

$$r_{ref} = min(|r_{ss}|,|r_{max}|).sgn(\delta)), \quad (39)$$
$$\beta_{ref} = \min(|\beta_{ss}|,|\beta_{max}|).sgn(\delta) \quad (40)$$

where r_{ss} is the steady state value and obtained as:

$$r_{ss} = \left(\frac{(l_f+l_r)V_x}{(l_f+l_r)^2 - 0.5mV_x^2\left(\frac{l_f}{C_{\alpha_r}} - \frac{l_r}{C_{\alpha_f}}\right)}\right)\delta \quad (41)$$

and r_{max} is the maximum allowable yaw rate at a given longitudinal velocity and friction coefficient, which is stated as:

$$r_{max} = \left|\frac{\mu g}{V_x}\right| \quad (42)$$

and, β_{ss} is the steady state value described as:

$$\beta_{ss} = \left(\frac{l_r(l_f+l_r) - 0.5mV_x^2(\frac{l_f}{C\alpha_r})}{(l_f+l_r)^2 - 0.5mV_x^2\left(\frac{l_f}{C\alpha_r} - \frac{l_r}{C\alpha_f}\right)} \right)\delta \quad (43)$$

β_{max} is the maximum allowable sideslip angle based on friction coefficient defined as:

$$\beta_{max} = arctan(0.02\mu g) \quad (44)$$

In the optimization problem of MPC, the control and state constraints are accordingly defined. The constraints on the steering angle are applied in such a way to realize the physical limits and defined as:

$$-\frac{\pi}{6} \leq \delta \leq \frac{\pi}{6} \quad (45)$$

The constraints on the front and rear differential braking are described as:

$$[M_{zf}] \leq M_{zf,max} \quad (46)$$

$$[M_{zr}] \leq M_{zr,max} \quad (47)$$

where,

$$M_{zf,max} = \frac{\mu L F_{z,fr}}{2}$$

$$M_{zr,max} = \frac{L}{2}\left(\mu F_{z,rr} \frac{L}{2\sqrt{(l_r^2 + \frac{L^2}{4})}} \right) \quad (48)$$

4. RESULTS AND DISCUSSIONS

A 2 DOF discrete mathematical model of the vehicle is developed with system parameter variations to achieve the yaw stability by designing an adaptive MPC. The parameters longitudinal velocity V_x and friction coefficient μ have a variation domain of [45, 85 km/h] and [0.4, 0.8], respectively. These variations are chosen in such a way to realize the practical situations of accelerating/braking/obstacle avoiding and wet/dry road surfaces. The vehicle parameters are mentioned in Table 1.

Table 1. Vehicle simulation parameters.

Parameter	Value
Mass	1111 kg
Distance of Front Axle from CG l_f	1.01 m
Distance of Rear Axle from CG l_r	1.56 m
Moment of Inertia along z axis I_z	2031 m^2

4.1. Simulation Results

The stability of the vehicle is studied with respect to many transient steering input maneuvers including J turn, single lane change, sine maneuver and double lane change. The most useful and widely exploited steering inputs are sine and DLC that generates a dynamics behavior of vehicle. In the following section, the obtained simulation results for two different widely used input steering angles with and without corrective yaw moments are explained to evaluate the performance of controller. Firstly, the LTI model is simulated, followed by the proposed LTV model based adaptive MPC. The simulation is performed in Matlab/Simulink environment.

4.1.1. Sine Maneuver

In this section, the response of the vehicle model with respect to the sine maneuver is observed. Fig. 6 depicts the yaw rate obtained for the LTI model. The reference yaw rate can be observed inside the stability limit. The actual yaw rate - for the parameters $\mu = 0.4\ and\ V_x = 40\ km/h$ - follows the reference values. If, the parameters are changed ($\mu = 0.4, 0.9\ and\ V_x = 80\ km/h$), the responses are seen as outside the limit as the value of the friction coefficient and longitudinal velocity have increased.

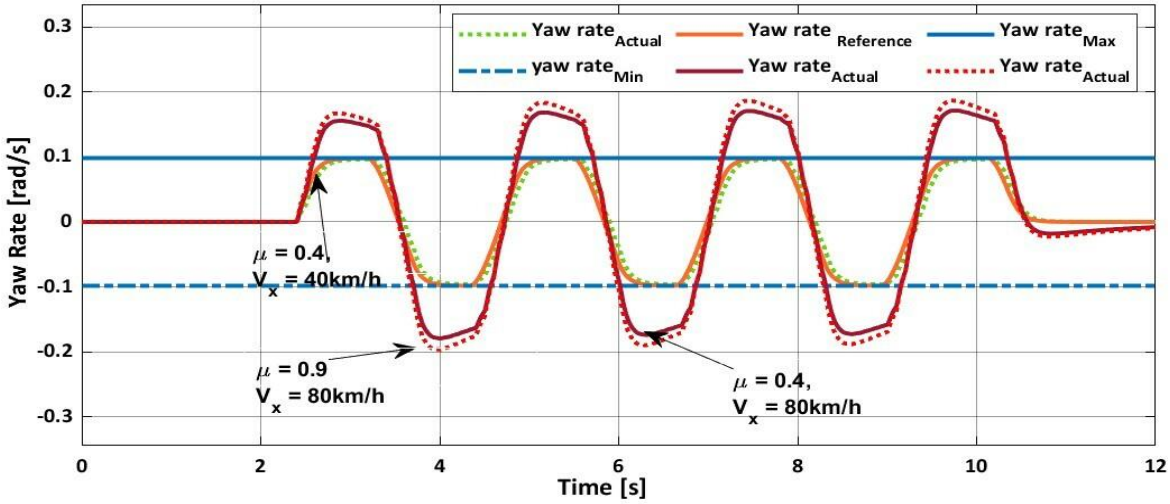

Fig. 6. Yaw rate for LTI model for sine steering.

Fig. 7 shows the reference (solid line) and calculated (dotted line) sine input steering angle. From the figure, it is observed that the calculated steering angle by MPC has a marginal error. The sine input with corrective yaw moment inputs is depicted in Fig. 8 for the LTV model. Fig. 8(a) represents the generated steering angle to bound the yaw rate inside the boundary limit. From Figs. 8(b) and (c), it is observed that the front and rear corrective yaw moments are added to the yaw motion of the vehicle for the time interval during which the gradient of yaw rate crossed the threshold value, respectively. The obtained moments are bound inside the limits defined by the input constraints in the opposite direction to negotiate the yaw rate.

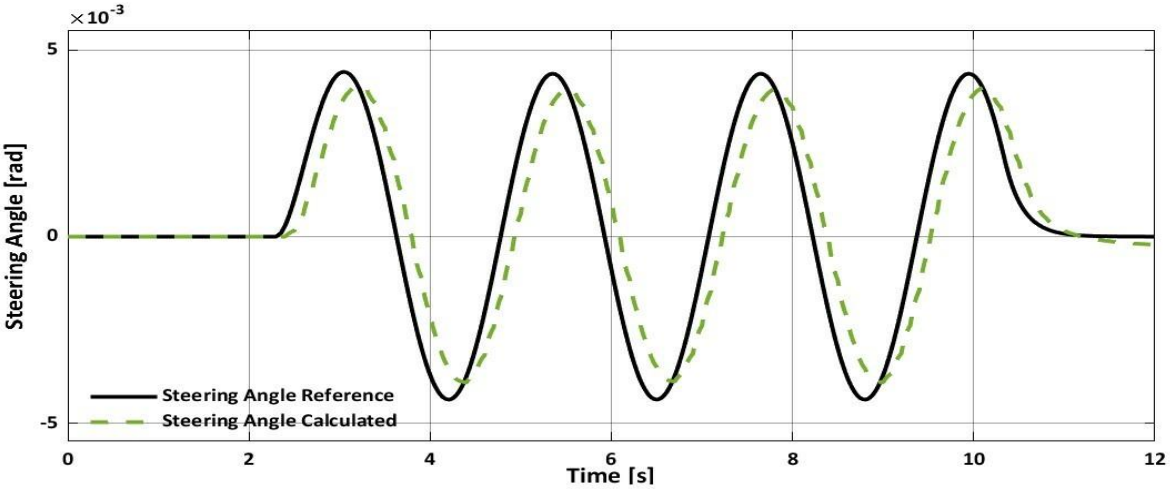

Fig. 7. The sine maneuver.

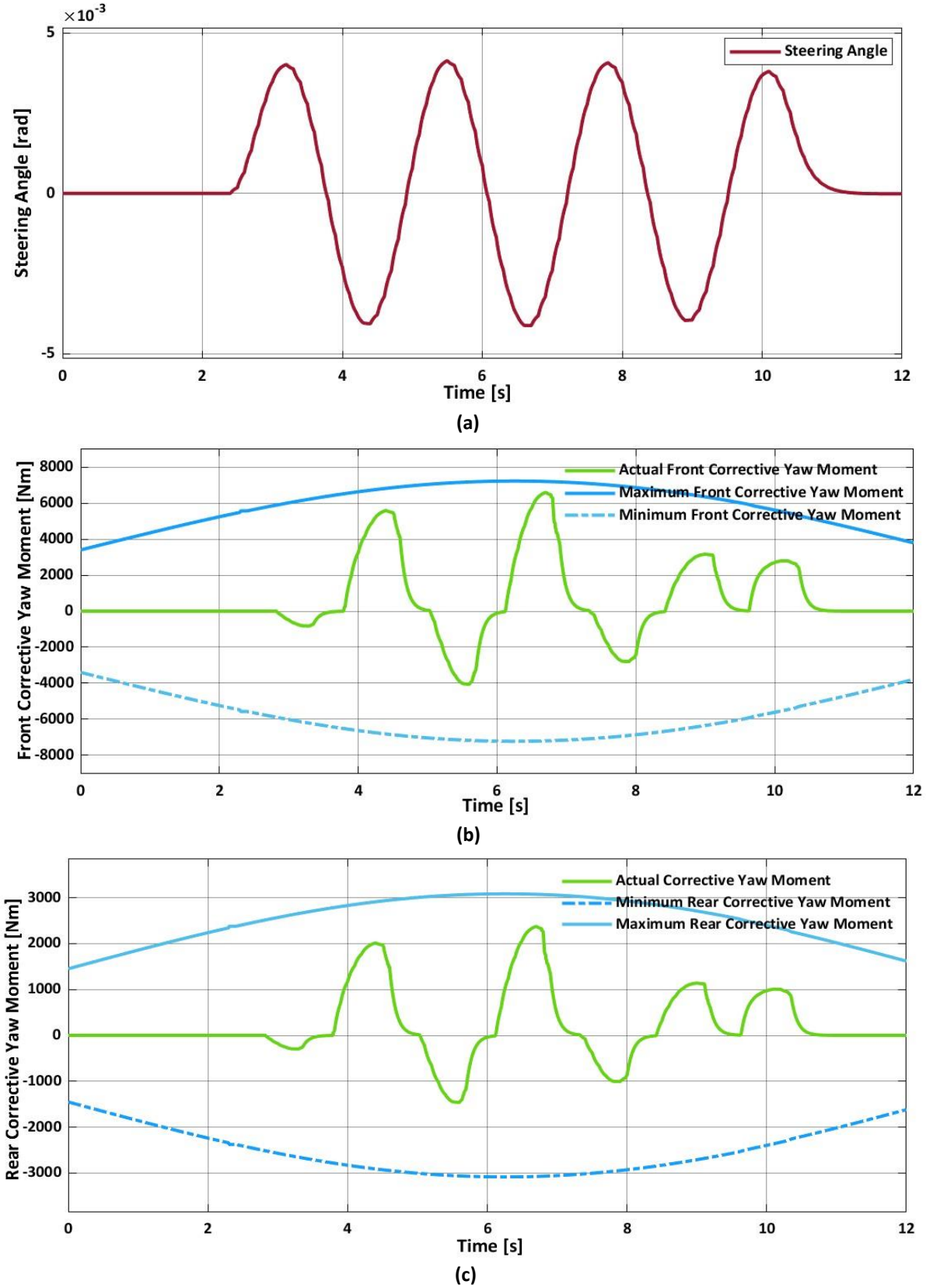

Fig. 8. Inputs for sine steering: a) steering angle; b) front corrective yaw moment; c) rear corrective yaw moment.

The yaw rate response of the sine input can be observed in Fig. 9. From the response, it can be analyzed that the tracked yaw rate has a marginal error but the peak values are achieved at the extreme values of the stability limit for front steering input without CYM. For

steering with the CYM, the yaw rate response is observed as oversteer since the peaks are decreased for the time duration for which the CYM is activated. The oversteer response of the vehicle is shown in Fig. 10 as $\alpha_f \leq \alpha_r$.

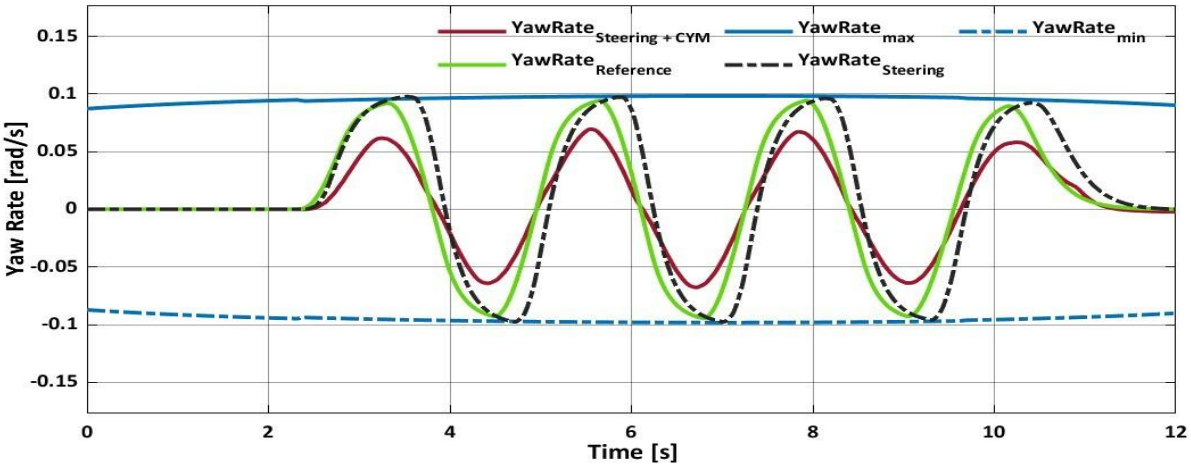

Fig. 9. Yaw rate for steering angle and CYM.

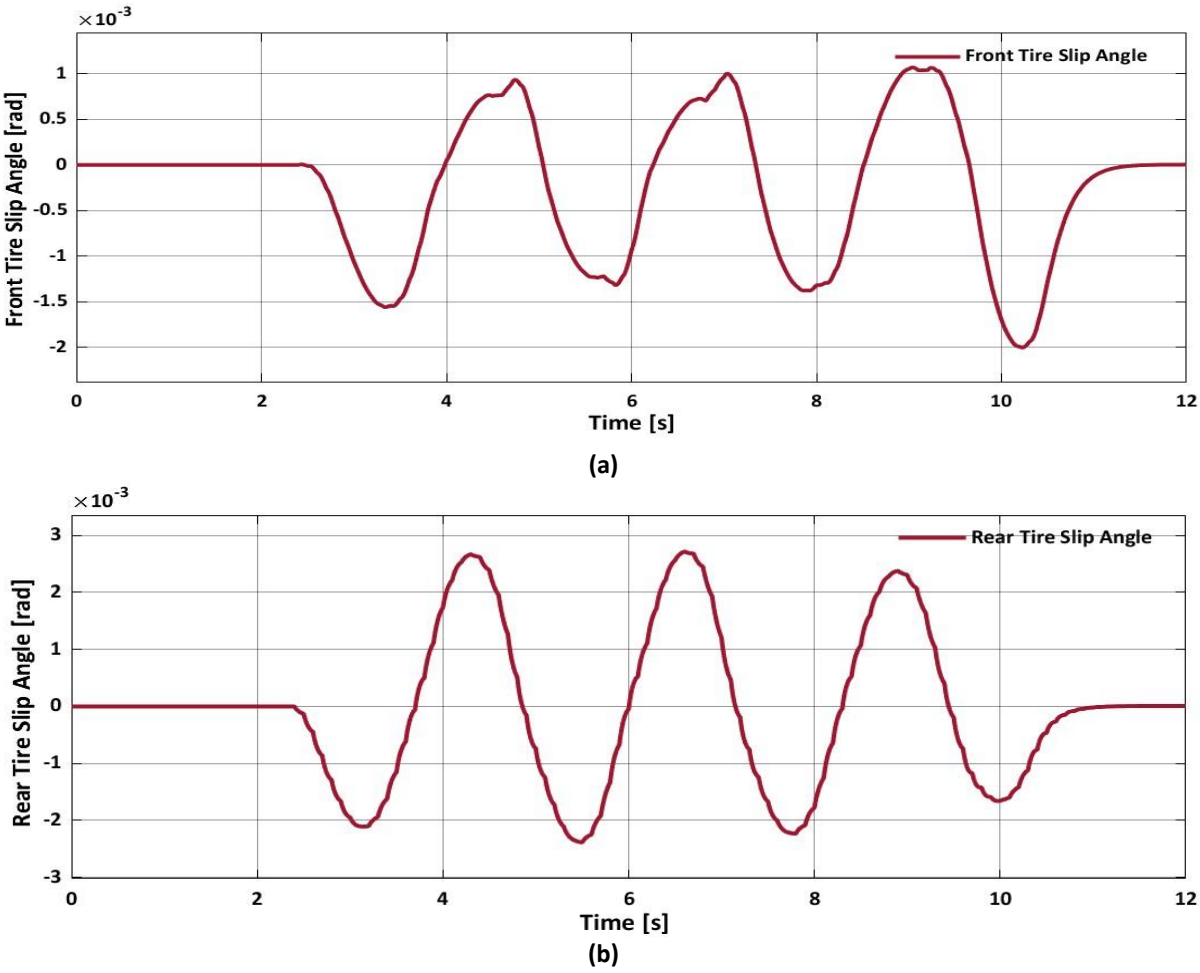

Fig. 10. Slip angle for sine steering: a) front tire slip angle; b) rear tire slip angle.

The lateral acceleration of the vehicle is bound within the limits as shown in Fig. 11. The AMPC has attained a feasible solution by minimizing the QP problem as in Fig. 12. The QP status value of 1 (positive integer) shows the feasibility of the problem in Fig. 13.

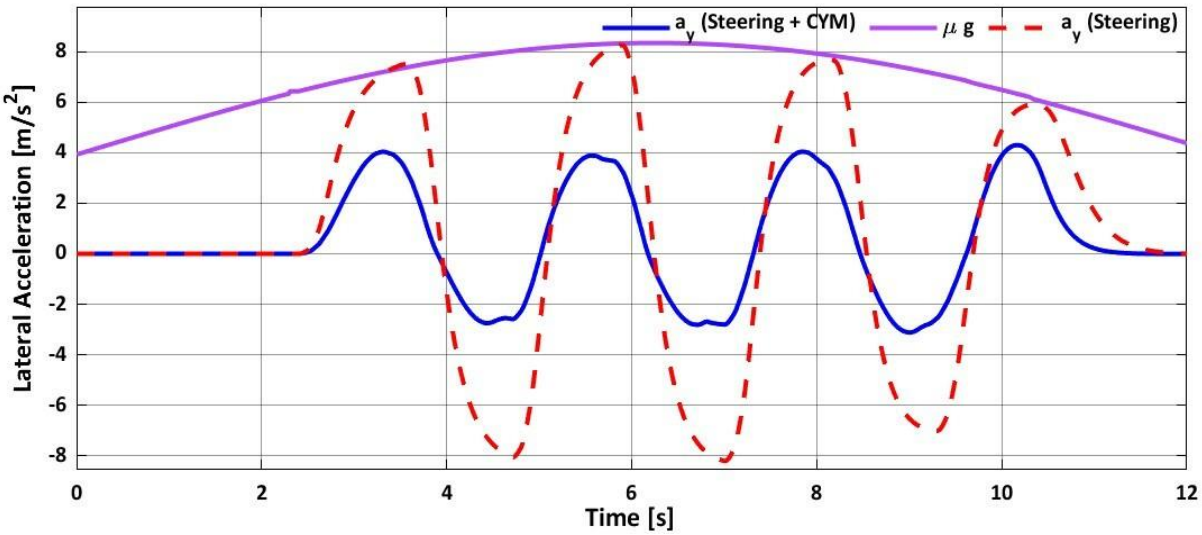

Fig. 11. Lateral acceleration response.

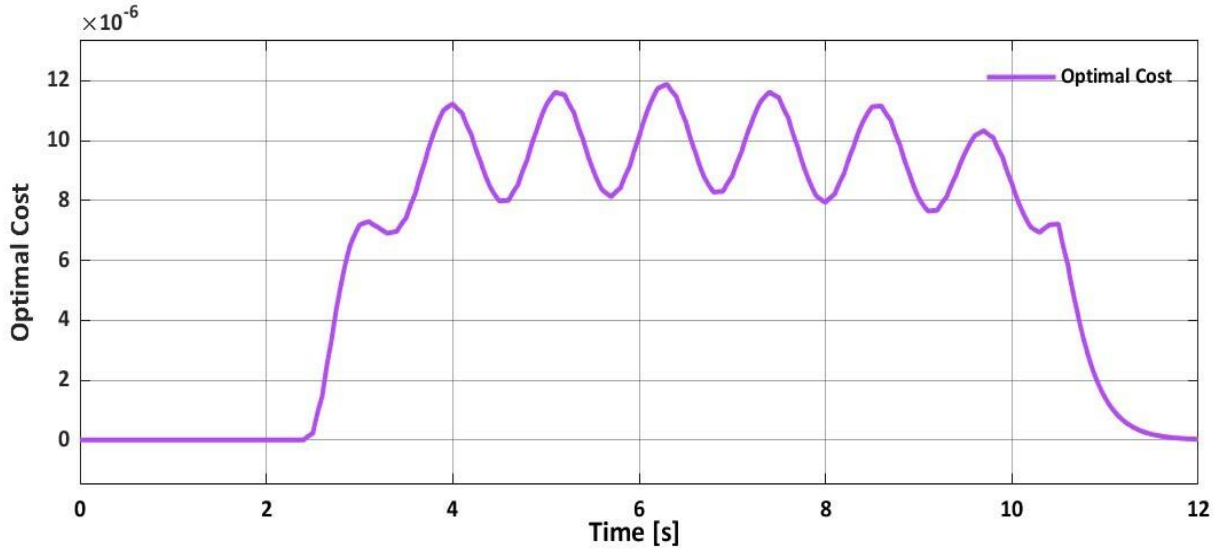

Fig. 12. Optimal cost.

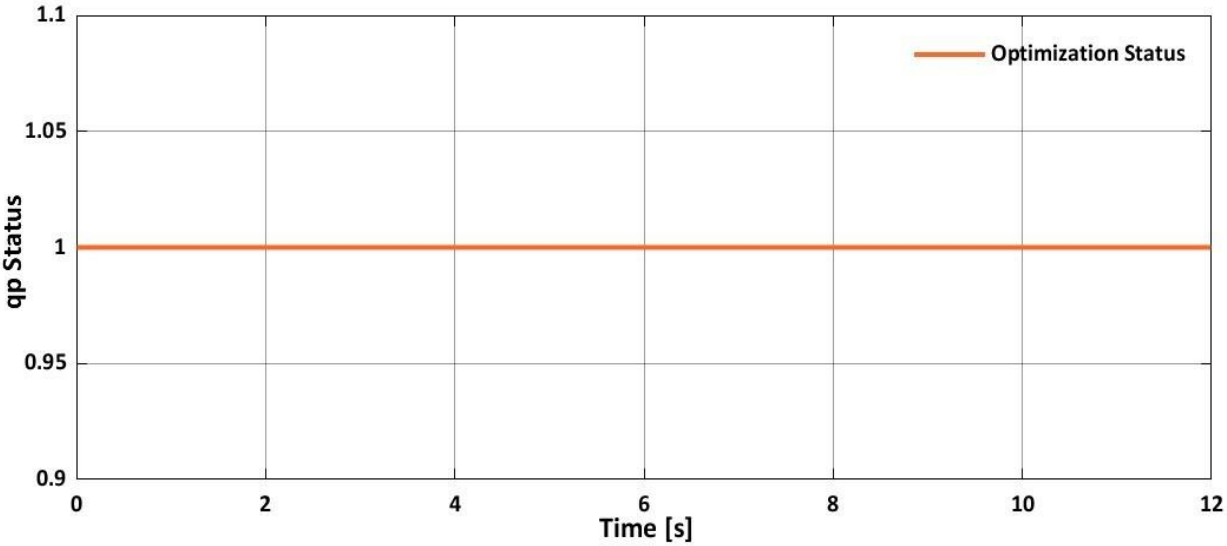

Fig. 13. QP status of AMPC problem.

4.1.2. Double Lane Change Maneuver

The input steering angle for the double lane change maneuver is shown in Fig. 14. From the figure, it is evident that, the input steering angle calculated by the comprises of a negligible difference with respect to the reference. The yaw rate response of the LTI model is shown in Fig. 15. The yaw rate obtained for an increased value of parameters ($\mu = 0.4, 0.9\ and\ V_x = 80\ km/h$) is observed to be outside the stability limit defined.

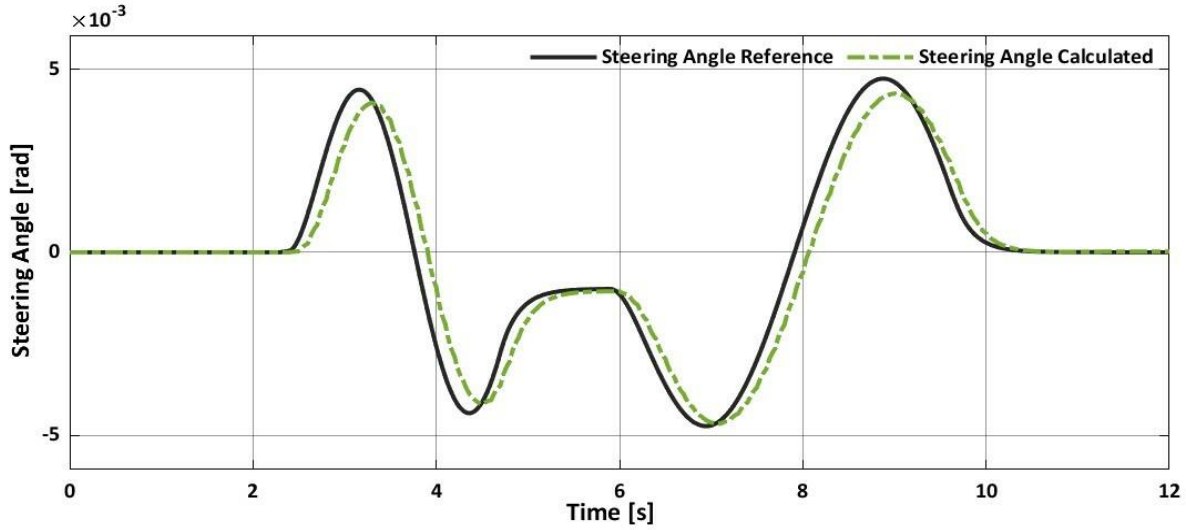

Fig. 14. Double lane change maneuver.

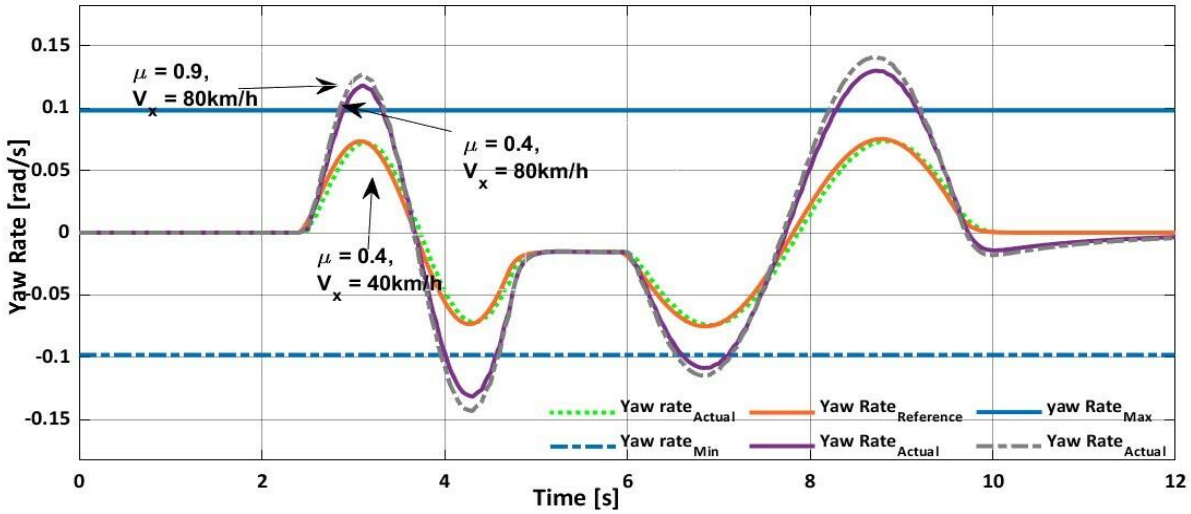

Fig. 15. Yaw rate response for DLC.

Fig. 16 shows the steering input with the front and rear corrective yaw moments. The front and rear corrective yaw moments are generated to improve the yaw stability by enforcing the yaw rate to be below the extreme values and bounding inside the stability limit. Fig. 17 shows the yaw rate response for steering angle with and without corrective yaw moments. The yaw rate is bound inside the limits and enforced below the extreme values. The yaw rate for steering with CYM attains the maximum values during the time interval $3s \leq t \leq 4s$, $8s \leq t \leq 10s$. The minimum values are attained for the time interval $4 \leq t \leq 5s$, $6s \leq t \leq 8s$. The yaw rate represented by the blue dotted line tracks the reference with a marginal error and attains the peak values at the stability limit for steering input only.

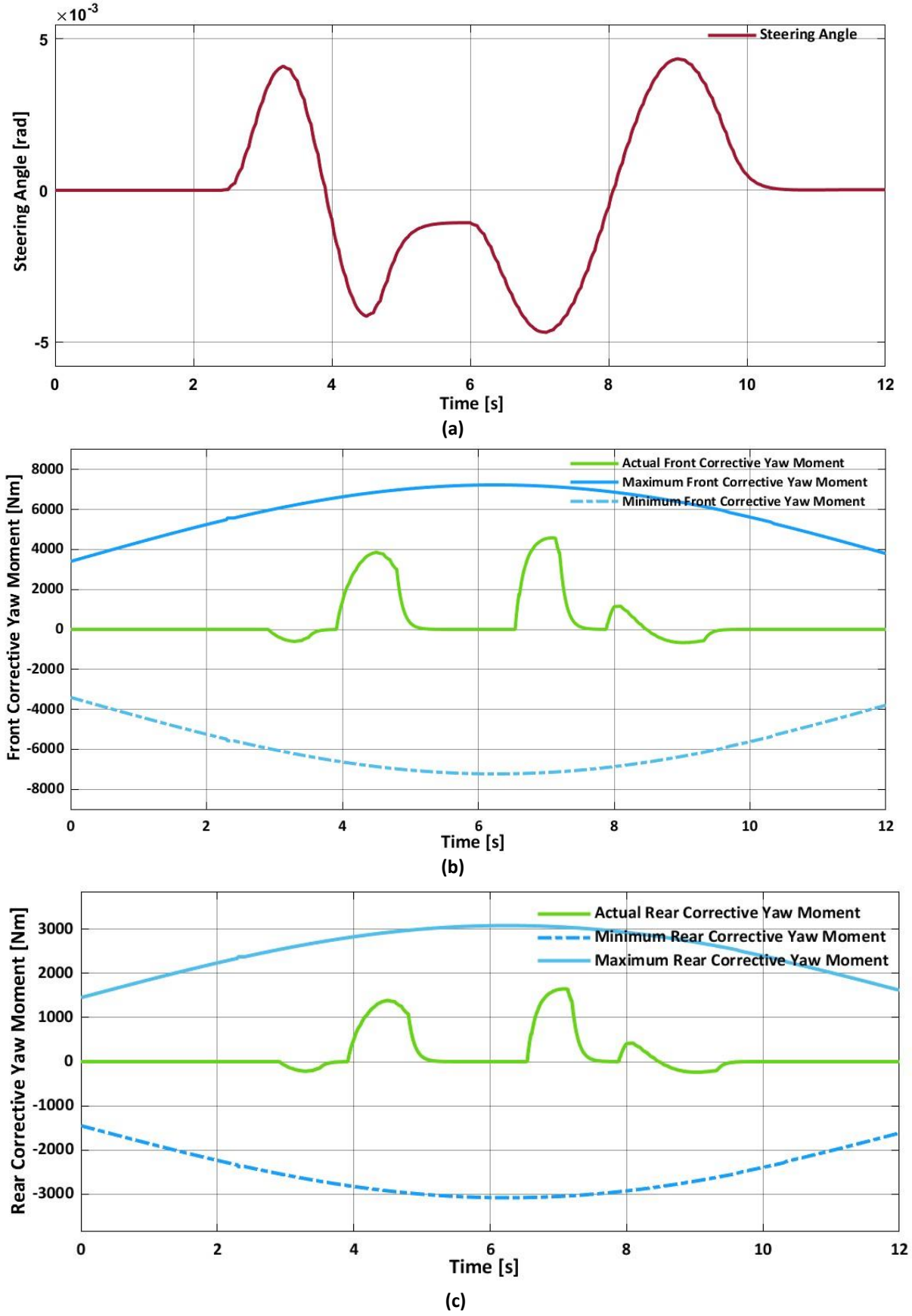

Fig. 16. Inputs for DLC: a) DLC steering; b) front corrective yaw moment rear; c) rear corrective yaw moment.

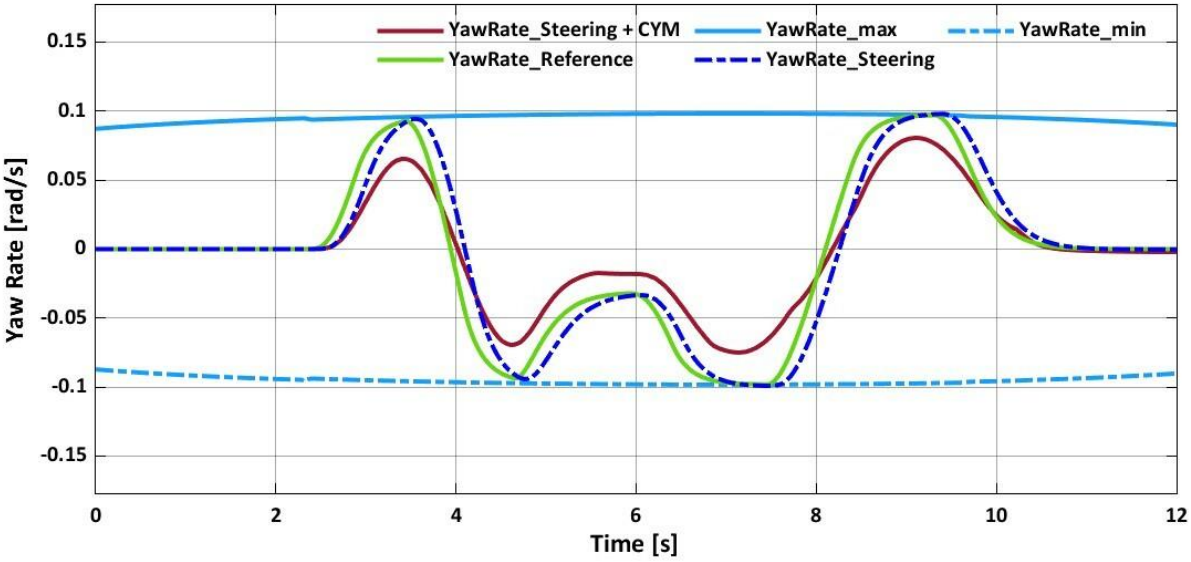

Fig. 17. Yaw rate response for DLC.

During the DLC maneuver, the lateral acceleration for steering input with and without CYM is shown in Fig. 18. It is evident that the lateral acceleration for steering with CYM inputs is less than as compared to only steering input and is bound inside the limit defined. The feasibility of the QP is shown in Fig. 19.

To evaluate the error between the steering input with and without CYM, the root mean square error (RMSE) is calculated by Eq. (49).

$$RMSE = \sqrt{mean(R - Y)^2} \tag{49}$$

where R is the reference value and Y represents the obtained value of the yaw rate. A RMSE of the obtained yaw rate (shown in Figs. 9 and 17) is calculated in Matlab for both steering inputs to show the improvement in yaw stability for the proposed methodology for the AMPC. Table 2 shows the RMSE of sine steering and double lane change steering for steering with and without CYM. From Table 2, it is can be seen that the activation of CYM has decreased the error between the reference and actual yaw rate.

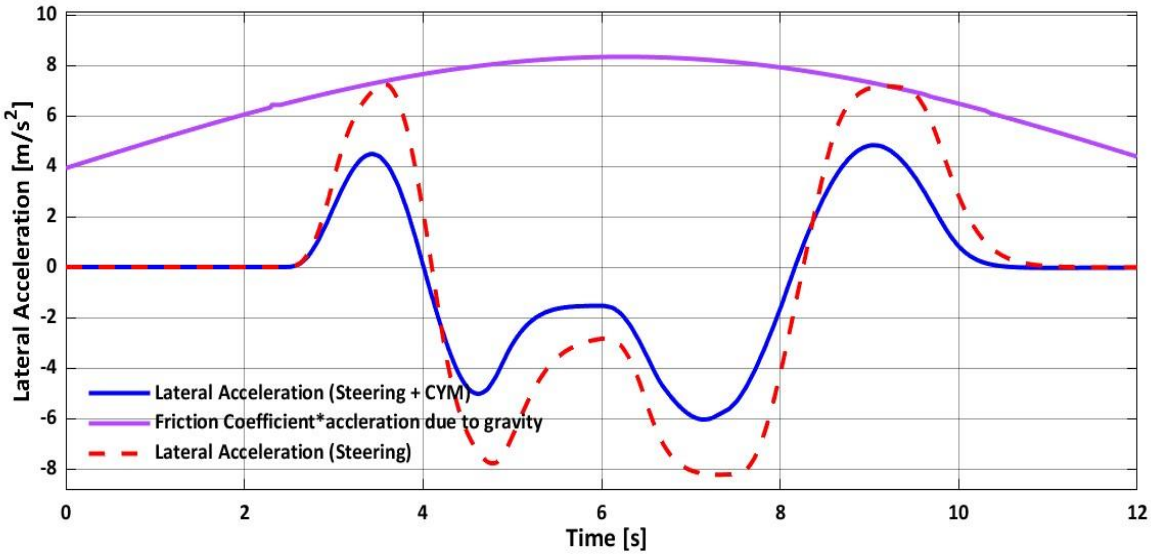

Fig. 18. Lateral acceleration response.

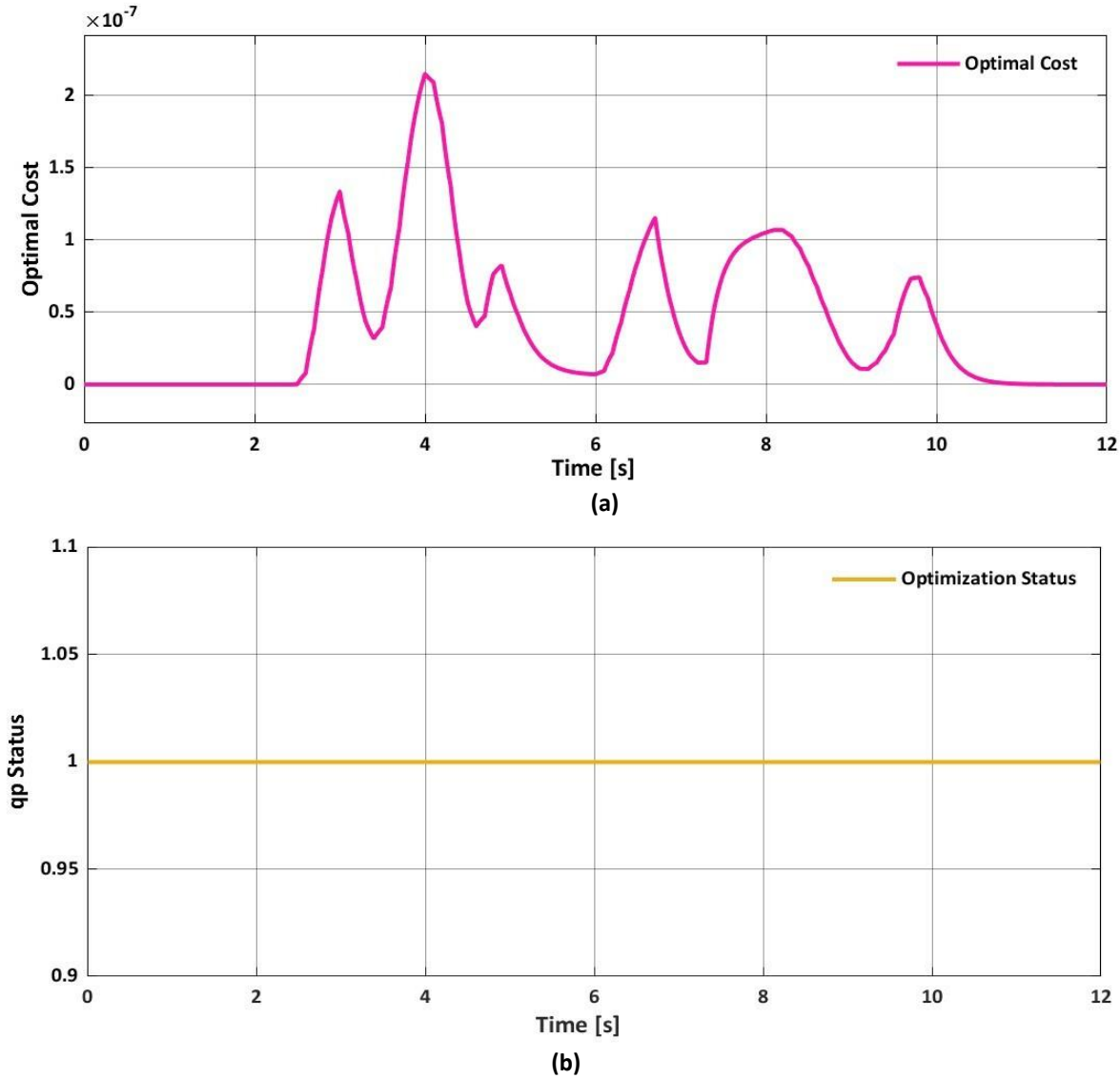

Fig. 19. Feasibility of AMPC: a) optimal cost; b) QP status of AMPC problem.

Table 2. RMSE of different steering inputs.

Steering input	RMSE
Sine steering input without CYM	0.0768
Sine steering input with CYM	0.0234
Double lane change steering input without CYM	0.0395
Double lane change steering input with CYM	0.0214

Further, a comparison between the proposed methodology with the previous state of the art is made to show that our method improves the yaw stability based on a 2 DOF bicycle model. In [2], the results section shows that the activation of differential braking to generate the corrective yaw moments occurs when the measured yaw rate crosses the bound to improve yaw stability. This may cause instability due to the presence of external disturbances. The method proposed in [5] for yaw stability comprises fluctuations at the peak values. These fluctuations show that the vehicle does not achieve a smooth cornering. In [16], the RMSE values obtained are high compared to our proposed method. Fig. 20 depicts the method applied in [2, 5], the dotted orange color line shows the measured yaw

rate generated for the methodology applied in [2]. It can be seen that the yaw rate is outside the stable limit during the time interval $4s \leq t \leq 6s$. The green dashed line shows the work done in [5] which comprises of fluctuations. The comparison graph is shown in Fig. 20, that depicts the proposed method in this paper has removed the fluctuations and achieved smooth cornering. The behavior of the yaw rate obtained depicts that the spinning of vehicle is avoided. Also, the yaw rate obtained is bounding inside the stability limit.

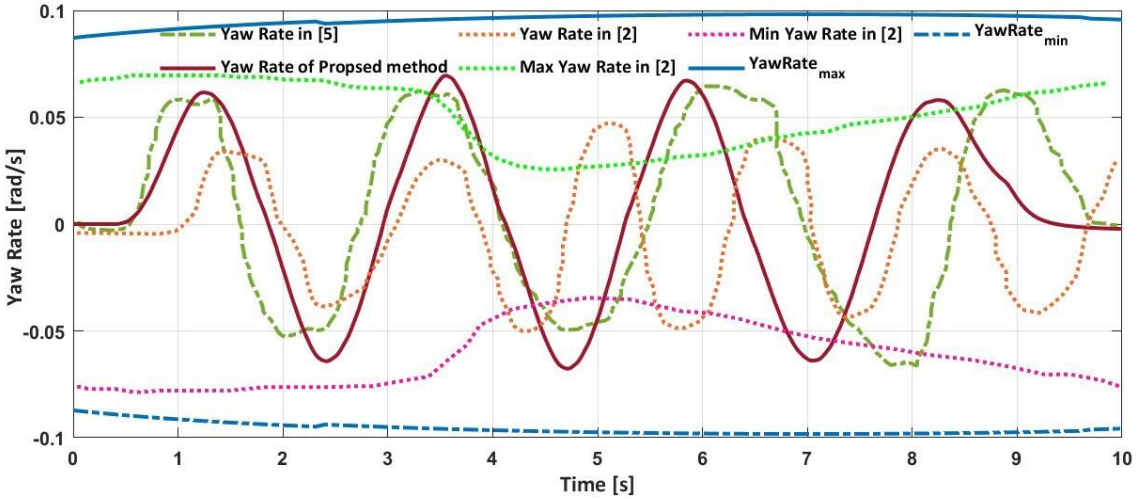

Fig. 20. Comparison of sine steering input.

The RMSE values obtained in [16] are also compared with our method as shown in Table 3. On comparing with other methods applied to improve the yaw stability, it is found that, the error obtained in [5, 16] are higher than our proposed method.

Table 3. RMSE comparison table with [5, 16].

Steering input	Methodology	RMSE Values
Sine Steering	Sine Steering Input without CYM	0.0768
	Sine Steering Input with CYM	0.0234
Sine Steering [5]	LTV-MPC	0.0573
Sine Steering [16]	AFS and DYC based SMC ($V_x = 33.8\frac{km}{h}, \mu = 0.8$)	5.552
	AFS and DYC based SMC ($V_x = 67.6\frac{km}{h}, \mu = 0.8$)	3.953

4.2. Discussions

Firstly, a MPC is developed for the LTI model considering the stability limits of the vehicle. For yaw stability, only the steering angle is implemented as an input in this LTI model. The controller is designed to operate at a specific value of longitudinal velocity and friction coefficient. Due to the invariant model, the controller is unable to handle the practical situations of changing parameters. The steering input is not able bound the yaw rate inside the stability limit. Therefore, an LTI model is not sufficient to overcome the problem highlighted in the research gap. For both the steering inputs, the LTI model-based controller is unable to bound the yaw rate inside the stability limit due to the change in parameters (V_x and μ) as the controller. Therefore, the yaw rate attains its peaks outside the extreme values of the boundary. The yaw rate response to steering input without CYM is prone to instability

due to achieving such extreme values. The lateral acceleration also achieves the verge of instability.

Further, an LTV MPC is developed to handle the changing vehicle dynamics for different dynamic steering inputs representing the driving scenario on roads, including sine steering and double lane change maneuver with and without activation of CYM. Figs. 8(b), 8(c), 16(b) and 16(c) respectively represent the activation of CYMs following the condition given by Eq. (17). For the gradient of yaw rate represented by the blue dotted line in Figs. 9 and 17, higher than the threshold value results in activation of CYMs for both sine and double lane change steering inputs. For the time interval $2.2s \leq t \leq 3.5s$ in Fig. 9, the value of gradient is found to be higher; therefore, for the same time duration CYMs attain the value are shown in Figs. 8(b) and 8(c). In Fig. 17, for the time duration $3.8s \leq t \leq 4.8s$, the value of CYMs in Figs. 16(b) and (c) increases, as the criteria for activation is satisfied. Therefore, for the different time intervals during which the criteria are satisfied, the CYMs are activated. The yaw rate for steering input with CYMs is represented in brown solid line in Figs. 9 and 17. It can be observed that due to the activation of CYMs, the yaw rate has decreased and is being enforced to remain inside the stability bounds. The CYM has considerably decreased the RMSE from 0.0768 and 0.0395 to 0.0234 and 0.0214 for sine and DLC steering, respectively.

For the proposed gradient based methodology for the LTV model-based AMPC controller, the obtained simulation results show improvement in the yaw stability as corrective yaw moments are added to the yaw motion of the vehicle shown by the brown solid line in Figs. 7 and 19. The yaw rate is bound below the peaks of reference, and thus avoids the verge of instability as obtained for steering without CYM. This bounding of yaw rate is achieved by activation of corrective yaw moments in the opposite direction of yaw rate upon the gradient threshold value is crossed. The gradient threshold value is crossed due to the variations in longitudinal velocity and friction coefficient. The lateral acceleration is also bounded below the boundary limits. Therefore, the steering angle with the corrective yaw moments shows better relative stability with respect to steering input without CYM. The RMSE describes the improvement in yaw stability by utilizing the proposed methodology for the AMPC. Fig. 20 shows the improvement of stability in the yaw rate in comparison to other methods in the literature. The RMSE value has decreased from 5.552, 3.953 in [16] and 0.0573 in [5] to 0.0234 for sine steering input by utilizing the proposed methodology.

The feasibility of the AMPC quadratic programming problem is analyzed by obtaining the QP status value of 1. The positive integer value shows the feasibility of the AMPC cost function for both types of inputs. This shows that the proposed AMPC method performs well by satisfying all the constraints.

5. CONCLUSIONS

In this work, a novel yaw rate gradient-based activation of corrective yaw moments (CYMs) as an input for an integrated actuator control approach to improve the yaw stability of the 2 DOF LTV model-based AMPC has been investigated. To include the practical scenarios of roads, friction coefficient and longitudinal velocity are chosen as parameters of interest to be varied. The profiles of both parameters are selected such that low friction

(wet or icy roads) combines with low velocity, and high friction (dry roads) engages with high velocity. From the simulation results, it is found that the performance of LTV model-based adaptive MPC with the proposed yaw rate gradient-based integrated control approach of steering angle with corrective yaw moments is better in comparison to steering input without CYMs and LTI model-based MPC with steering input actuation. The understeer response is brought down to oversteer due to the presence of corrective yaw moments; thus achieving a higher stability margin in comparison to steering without CYMs. By comparing with the previous state of the art, it is found that the proposed method has improved the yaw stability by removing fluctuations in the yaw rate, and the obtained values of CYMs bound the yaw rate inside the stability limit. Thus, resulting in avoiding the spinning of the vehicle during the cornering maneuvers opted. This technique prevents the vehicle from accidents at corners of roads or in hilly areas. The QP problem formulated with the given number of constraints for the AMPC is found to be feasible for both inputs including the sine and double lane change maneuver.

The proposed method is limited to the smaller tire slip angle and with a linear approximation of the tire model. The implemented controller is an adaptive MPC; therefore, the required vehicle model should be a linear time varying model. The obtained yaw rate comprises a stability margin, due to which the effect of disturbance does not drive the yaw rate outside the stability limits. The future scope of this work is to include finding the optimal stability margin, higher slip angle of tires, and varying other parameters of interest to analyze the effect on stability.

Acknowledgement: Authors would like to thank the National Institute of Technology Patna, Bihar, India for providing the platform for research.

REFERENCES

[1] R. Rajamani, *Vehicle Dynamics and Control*, Springer Science & Business Media, 2011.

[2] R. Hajiloo, A. Khajepour, A. Kasaiezadeh, S. Chen, B. Litkouhi, "A model predictive control of electronic limited slip differential and differential braking for improving vehicle yaw stability," *IEEE Transactions on Control Systems Technology,* vol. 31, no. 2, pp. 797-808, 2023.

[3] W. Botes, T. Botha, P. Els, "Real-time lateral stability and steering characteristic control using non-linear model predictive control," *Vehicle System Dynamics,* vol. 61, no. 4, pp. 1063–1085, 2023.

[4] C. Jing, H. Shu, R Shu, Y. Song, "Integrated control of electric vehicles based on active front steering and model predictive control," *Control Engineering Practice,* vol. 121, pp. 105066, 2022.

[5] S. Li, X. Wang, G. Cui, X. Lu, B. Zhang, "Yaw and lateral stability control based on predicted trend of stable state of the vehicle," *Vehicle System Dynamics*, vol. 61, no. 1, pp. 111–127, 2022.

[6] W. Wenjuan, L. Shaobo, L. Caixia, "Adaptive coordinated stability control of vehicle considering stability margin," IEEE *33rd Chinese Control and Decision Conference,* pp. 5191-5196, 2021.

[7] S. Li, Z. Yang, "AFS/DYC control of in-wheel motor drive electric vehicle with adaptive tire cornering stiffness," *IEEE 6th CAA International Conference on Vehicular Control and Intelligence,* pp. 1-6, 2022.

[8] S. Cairano, H. Tseng, D. Bernardini, A. Bemporad, "Vehicle yaw stability control by coordinated active front steering and differential braking in the tire sideslip angles domain," *IEEE Transactions on Control Systems Technology,* vol. 21, no. 4, pp. 1236–1248, 2012.

[9] N. Ahmadian, A. Khosravi, P. Sarhadi, "Driver assistant yaw stability control via integration of AFS and DYC," *Vehicle System Dynamics,* vol. 60, no. 5, pp. 1742-1762, 2022.

[10] R. Hajiloo, M. Abroshan, A. Khajepour, A. Kasaiezadeh, S. Chen, "Integrated steering and differential braking for emergency collision avoidance in autonomous vehicles," *IEEE Transactions on Intelligent Transportation Systems,* vol. 22, no. 5, pp. 3167-3178, 2021.

[11] Q. Cui, R. Ding, X. Wu, B. Zhou, "A new strategy for rear-end collision avoidance via autonomous steering and differential braking in highway driving," *Vehicle System Dynamics,* vol. 58, no. 6, pp. 955–986, 2019.

[12] H. Her, Y. Koh, E. Joa, K. Yi, K. Kim, "An integrated control of differential braking, front/rear traction, and active roll moment for limit handling performance," *IEEE Transactions on Vehicular Technology,* vol. 65, no. 6, pp. 4288-4300, 2015.

[13] J. Feng, S. Chen, Z. Qi, "Coordinated chassis control of 4wd vehicles utilizing differential braking, traction distribution and active front steering," *IEEE Access,* vol. 8, pp. 81055–81068, 2020.

[14] P. Wang, Z. Liu, Q. Liu, H. Chen, "An mpc-based manoeuvre stability controller for full drive-by-wire vehicles," *Control Theory and Technology,* vol. 17, no. 4, pp. 357-366, 2019.

[15] H. Nam, W. Choi, C. Ahn, "Model predictive control for evasive steering of an autonomous vehicle," *International Journal of Automotive Technology,* vol. 20, no. 5, pp. 1033-1042, 2019.

[16] M. Lu, Z. Xu, "Integrated handling and stability control with AFS and DYC for 4wid-evs via dual sliding mode control," *Automatic Control and Computer Sciences,* vol. 55, no. 3, pp. 243-252, 2021.

[17] Y. Song, H. Shu, X. Chen, S. Luo, "Direct-yaw-moment control of four wheel-drive electrical vehicle based on lateral tyre road forces and sideslip angle observer," *IET Intelligent Transport Systems,* vol. 13, no. 2, pp. 303-312, 2019.

[18] Y. Zhu, H. Li, K. Wang, Y. Bao, P. Zeng, "A simulation study for lateral stability control of vehicles on icy asphalt pavement," *Journal of Advanced Transportation*, vol. 2022, pp. 1-15, 2022.

[19] J. Wang, S. Liu, J. Wu, J. Yang, A. Li, "Research on model predictive control method for vehicle lateral stability based on hardware-in-the-loop test," *Mathematical Problems in Engineering,* vol. 2020, pp. 1-11, 2020.

[20] S. Li, G. Wang, B. Zhang, Z. Yu, G. Cui, "Vehicle yaw stability control at the handling limits based on model predictive control," *International Journal of Automotive Technology,* vol. 21, no. 2, pp. 361-370, 2020.

[21] H. Termous, H. Shraim, R. Talj, C. Francis, A. Charara, "Coordinated control strategies for active steering, differential braking and active suspension for vehicle stability, handling and safety improvement," *Vehicle System Dynamics,* vol. 57, no. 10, pp. 1494-1529, 2019.

[22] Y. Lu, J. Linag, G. Yin, J. Feng, F. Wang, L. Xu, "Torque vector compensation strategy with adaptive model predictive control considering steering actuator fault," *IEEE Proceedings of the 2022 6th CAA International Conference on Vehicular Control and Intelligence*, pp. 1-6, 2022.

[23] H. Wang, L. Zhao, W. Chen, X. Liang, "Segmented coordinated control based on active steering and differential braking for lane departure prevention," *IEEE Proceedings of the 2020 4th CAA International Conference on Vehicular Control and Intelligence*, pp. 163-168, 2020.

[24] J. Tavoosi, "Stable backstepping sliding mode control based on ANFIS2 for a class of nonlinear systems," *Jordan Journal of Electrical Engineering*, vol. 6, no. 1, pp. 49-62, 2020.

[25] S. Yordanova, M. Slavov, "Stability analysis of model-free adaptive fuzzy logic control system applied for liquid level control in soda production," *Jordan Journal of Electrical Engineering*, vol. 9, no. 1, pp. 14-30, 2023.

[26] H. Pacejka, *Tire and Vehicle Dynamics,* Elsevier, 2005.

[27] W. Chen, D. Tan, L. Zhao, "Vehicle sideslip angle and road friction estimation using online gradient descent algorithm," *IEEE Transactions on Vehicular Technology,* vol. 67, no. 12, pp. 11475-11485, 2018.

[28] L. Wang, *Model Predictive Control System Design and Implementation using MATLAB®*, Springer Science & Business Media, 2009.

[29] J. Ji, A. Khajepour, W. Melek, Y. Huang, "Path planning and tracking for vehicle collision avoidance based on model predictive control with multi-constraints," *IEEE Transactions on Vehicular Technology,* vol. 66, no. 2, pp. 952-964, 2016.

[30] S. Cheng, L. Li, H. Guo, Z. Chen, P. Song, "Longitudinal collision avoidance and lateral stability adaptive control system based on mpc of autonomous vehicles," *IEEE Transactions on Intelligent Transportation Systems,* vol. 21, no. 6, pp. 2376-2385, 2019.

[31] A. Dhar, S. Bhasin, "Adaptive mpc for uncertain discrete-time LTI MIMO systems with incremental input constraints," *IFAC,* vol. 51, no. 1, pp. 329-334, 2018.

[32] C. Jia, W. Qiao, J. Cui, L. Qu, "Adaptive model-predictive-control based real-time energy management of fuel cell hybrid electric vehicles," *IEEE Transactions on Power Electronics,* vol. 38, no. 2, pp. 2681-2694, 2022.

[33] M. Turki, N. Langlois, A. Yassine, "An analytical tuning approach for adaptive MPC parameters applied to LTV SISO systems," *IEEE 2018 Annual American Control Conference*, pp. 1534-1539, 2018.